
Article:
Zeng, X. orcid.org/0000-0003-4896-8080, Poppe, S., Lehmann, A. et al. (6 more authors) (2019) A self-assembled bicontinuous cubic phase with a single-diamond network. Angewandte Chemie International Edition, 58 (22). pp. 7375-7379. ISSN 1433-7851

https://doi.org/10.1002/anie.201902677

A Self-assembled Bicontinuous Cubic Phase with Single Diamond Network

Xiangbing Zeng,[a†] Silvio Poppe,[b†] Anne Lehmann,[b] Marko Prehm,[b] Changlong Chen,[c] Feng Liu[c,*], Huanjun Lu,[a,‡] Goran Ungar,[a,c,*] Carsten Tschierske[b,*]

[a] Department of Materials Science and Engineering, University of Sheffield, Sheffield S1 3JD, U.K.

[b] Institute of Chemistry, Martin-Luther-University Halle-Wittenberg, Kurt-Mothes-Straße 2, 06120 Halle.

[c] State Key Laboratory for Mechanical Behaviour of Materials, Xi'an Jiaotong University, Xi'an 710049 (P.R. China)

Abstract: We report the first single diamond cubic phase in a liquid crystal. This skeletal structure with $Fd\bar{3}m$ space group is formed by self-assembly of bolaamphiphiles with swallow-tailed lateral chains. It consists of bundles of π-conjugated *p*-terphenyl rods fused into an infinite network by hydrogen-bonded spheres at tetrahedral four-way junctions. We also present a quantitative model relating molecular architecture with space-filling requirements of six possible bicontinuous cubic phases, i.e. single- and double-network versions gyroid, diamond and "plumbers nightmare".

Among the most intriguing self-assembled nano- and mesoscale soft matter structures are the cubic phases formed by lyotropic and thermotropic liquid crystals (LCs), by block copolymers [1,2] and by nano-particle arrays. [3,4,5] Two classes of cubic phases can be distinguished, the "bicontinuous" and the "micellar" types.[6,7] The micellar phases represent periodic arrays of spheres on a cubic lattice, whereas the bicontinuous phases are more complex and usually formed by two networks divided by a minimal surfaces with constant mean curvature. Depending on the symmetry, the double gyroid (DG, $Ia\bar{3}d$, Q^{230}), the double diamond (DD; $Pn\bar{3}m$, Q^{224}) and the body centered plumbers nightmare ("double primitive") cubic phases; DP; $Im\bar{3}m$, Q^{229}) with valencies of the junctions being $\nu = 3$, 4 and 6, respectively, can be distinguished (Fig. 1a-c).

† Authors contributed equally

‡ Present address: College of Chemistry, Chemical Engineering and Materials Science, Soochow University, Suzhou, China

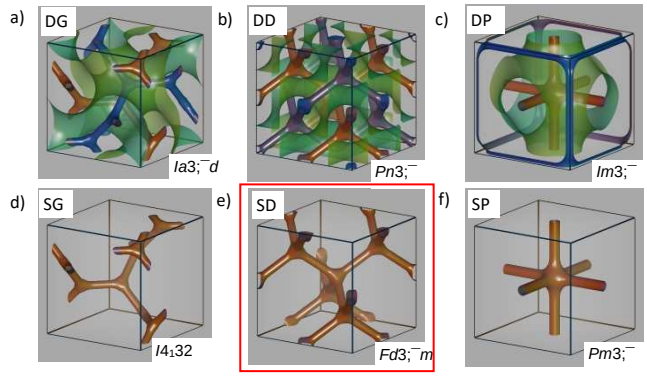

Figure 1. a-c) The three double network cubic phases with their infinite minimal surfaces (green) separating the two networks and d-f) the corresponding single networks [8] with abbreviations and corresponding space groups. The space groups in a-c) refer to structures where the two networks are identical (brown = blue); were they different (alternating double networks), the space group would be the same as in the corresponding single networks.

In contrast to these double network structures, there is also a structure formed by three networks[9] and the corresponding structures composed of only one network (SG = $I4_132$, Q^{214}; SD = $Fd\bar{3}m$, Q^{227}; and SP = $Pm\bar{3}m$, Q^{221} see Fig. 1d-f). The latter three are extremely rare and only known as solid-state structures, whereas they are considered as metastable in soft matter. They are of special interest for their extraordinary photonic properties;[10,11] e.g. the single gyroid (Fig. 1d) and the single diamond (Fig. 1e) were found responsible for the structural color of biophotonic structures in butterfly wing scales and some beetle shells.[12,13] Due to their unique photonic properties they are of special interest for metamaterials and other photonic applications.[11, 14] Solid state single network structures have been produced by holographic lithography or by selective deposition using a double network template,[14,15,16] but no direct formation of a single network in a strict bottom-up self-assembly process has been reported so far. Only the so-called alternating double network DG structure in which the two networks are different and which therefore has the same space groups $I4_132$ as the related single network structure has been reported for ABC triblock copolymers.[14,17] Neither a related alternating DD structure, nor the SD structure (Fig. 1e), both with $Fd\bar{3}m$ symmetry, have yet been reported in self-assembled soft matter.

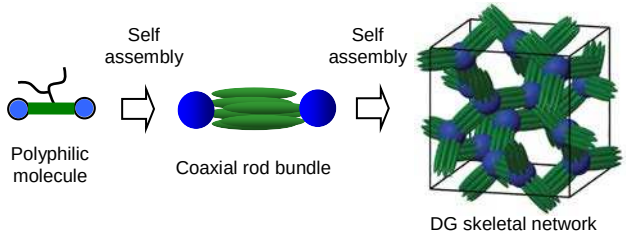

Figure 2: Self-assembly of polyphilic rods into coaxial bundles and liquid crystalline networks.

Here we report the first example of a liquid crystalline (LC) single diamond network phase with space group $Fd3;^{-}m$, self-assembled from bottom up and belonging to the so-called coaxial rod-bundle phases.[18,19,20,21] These phases were found for π-conjugated rod-like molecules with sticky ends (e.g. glycerols) and bulky alkyl or perfluoroalkyl chains attached to one of the sides (Fig. 2, left). The π-conjugated rods form bundles (Fig. 2, middle) which are interconnected by two-, three- or four-way junctions. Whereas two-way junctions lead to infinite chains (columns) which organize on a hexagonal lattice,[21] three- or four-way junctions give rise to the DG network ($Ia3;^{-}d$, Fig. 2, right)[18,20] and the DD network ($Pn3;^{-}m$),[19] respectively. In all cases the lateral chains fill the space between the columns or networks. In the double network structures the number of consecutive bundles between the junctions is limited to integer numbers, either two[18,19] or only one.[20] In order to obtain new types of rod bundle phases compounds **1/14** - **1/22** with swallow tailed lateral alkyl chain, shown in the formula in Tab. 1, have been synthesized as described in the Supporting Information (Scheme S1). The observed phase sequences and transition temperatures are collated in Table 1.

Table 1: Molecular structure and phase transition temperatures of compounds **1/*n***.[a]

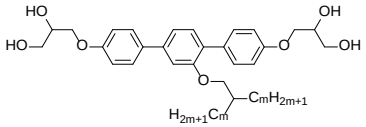

1/*n*	*T*/°C [Δ*H*/kJmol^{-1}]	a_{cub} /nm (*T*/°C)
1/12	Cr 82 [8.1] *p2* 118 [2.3] $Ia3;^{-}d$ 143 [1.3] Iso	7.73 (130)
1/14	Cr 104 [30.8] Lam_{Sm} 108 [2.2] $Ia3;^{-}d$ 161 [1.3] Iso	7.71 (130)
1/16	Cr 78 [18.6] Lam_{Sm} 114 [4.0] $Ia3;^{-}d$ 160 [2.1] Iso	7.71 (120)
1/18	Cr 65 [12.8] Lam_{Sm} 104 [3.4] $Fd3;^{-}m$ 136 [0.7] Iso	6.39 (110)
1/20	Cr 54 [42.9] $Fd3;^{-}m$ 160 [2.7] Iso	6.32 (150)
1/22	Cr 61 [51.7] $Fd3;^{-}m$ 172 [3.9] Iso	6.32 (160)

[a] determined by DSC second heating scan, 10 Kmin^{-1}. Abbreviations: Cr = crystalline solid, $Fd3;^{-}m$ = SD cubic phase with $Fd3;^{-}m$ symmetry; $Id3;^{-}d$ = DG cubic phase with $Id3;^{-}d$ symmetry; *p*2 = honeycomb LC phase with *p*2 lattice;[22] Lam_{Sm} = lamellar phase with coplanar bundles and periodicity in the layers;[23] Iso = isotropic liquid; for DSCs, see Fig. S1, Tables with XRD data, see Tables S1 and S2.

On cooling from the isotropic liquid state a sudden increase in viscosity, associated with a transition enthalpy of 2.2-4.0 kJ mol^{-1} is observed for all **1/*n*** compounds, though the samples remain optically isotropic. This is a first indication of the formation of a cubic phase. For compounds **1/12-1/18** this cubic phase is replaced by an additional birefringent LC phase on further cooling, whereas the long chain compounds **1/20** and **1/22** crystallize; herein the focus is exclusively on the cubic phases. The LC nature of the isotropic mesophases was confirmed

by the diffuse scattering in the WAXS region with a maximum around d = 0.46–0.47 nm (see insets in Fig. 3 and Fig. S4d). This indicates that the individual molecules do not have fixed positions and therefore only a mean distance is recorded.

For compounds **1/12-1/16** the SAXS pattern can be indexed to a cubic phase with space group $Ia\bar{3}d$ and a_{cub} around 7.6 nm, being in line with a DG structure formed by bundles of rods, with junctions one molecular length apart (see Figs. 3, S2, S3 and Table S1).[20] As the length of the side-chains is increased in compounds **1/18-1/22**, the SAXS pattern changes. The series of sharp reflections with 1/d-values in the ratio √3: √8: √11: √12: √16: √19…etc. can again be indexed to a cubic phase, but this time with space group $Fd\bar{3}m$ and with the lattice parameter a_{cub} = 6.39 nm (see Figs. 3, S4 and Table S2). From **1/18** to **1/22** (Table 1) a_{cub} remains almost unchanged, in agreement with the proposed network structure with fixed inter-junction distance; any increase in molecular volume can be compensated by a reduction in the average number of molecules in a bundle. Electron density (ED) maps, constructed from diffraction intensities, are shown in Fig. 4. The method of selecting the correct phase combination is described in Section 2.3 of SI. Note that correct selection was facilitated here by being able to compare ED histograms of members of a homologous series of compounds (here **1/18** and **1/22**), i.e. applying a version of the isomorphous replacement technique.[24] In Fig. 4 the green isoelectron surface encloses the high ED space, filled mainly by the aromatic cores and the glycerol groups, while the low density region (orange/red) contains the branched alkyl chains. The ED maps clearly show a single network with tetrahedral four-way junctions, as expected for a single diamond net (Fig. 4a). The low ED (red to orange) between the networks confirms the absence of a second intercalated network (Fig. 4b).

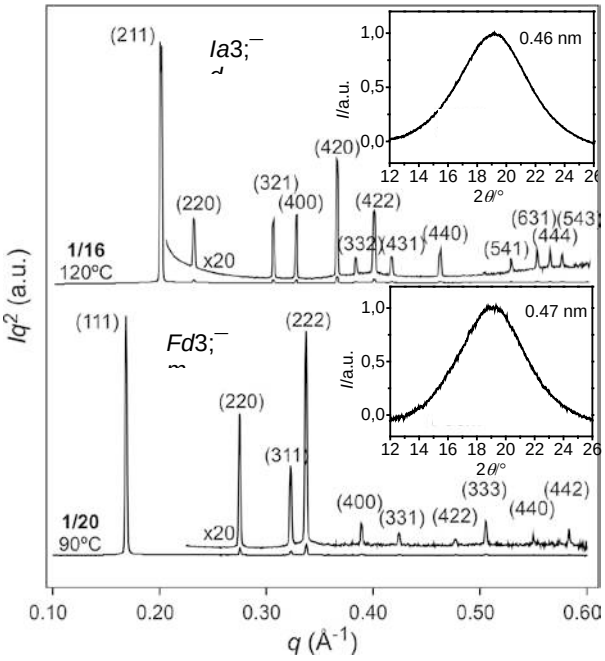

Figure 3: Representative SAXS patterns with indexation; top: *Ia*3;¯*d* phase (DG) of **1/16** and bottom: *Fd*3;¯*m* phase (SD) of **1/20**), the insets show the corresponding WAXS (see also Fig. S4d).

As the distance between the junctions in a SD structure is $(3^{1/2}\ a_{cub})/4 \approx 2.77$ nm,[25] which is only slightly larger than the measured molecular length between the ends of the glycerol groups (L_{mol} = 2.50 nm),[20,22] it follows that a network segment contains a single molecular bundle. That the distance between junctions is slightly longer than the molecular length is due to the relatively large size of the spheres formed by 4x10=40 glycerol units

Furthermore, the total number of molecules in a unit cell n_{cell} is calculated according to $V_{cell}/V_{mol} = a_{cub}^3/V_{mol}$ where V_{mol} is molecular volume (for calculation see SI). For **1/18** we obtain $n_{cell} \approx 157$. Considering that a unit cell contains 16 network segments, each bundle contains about 10 (9.8) molecules (Table S4). This value is close to the value of about 12 molecules side-by-side in a bundle that was reported for the DG and DD type skeletal cubic phases, including the DG phase of compounds **1/12-1/16** (Table S3).[18,19,20,21] Similar values were also obtained for **1/20** and **1/22** (see Table S4). Thus, the formation of a cubic phase with a single diamond network consisting of single bundle segments is confirmed.

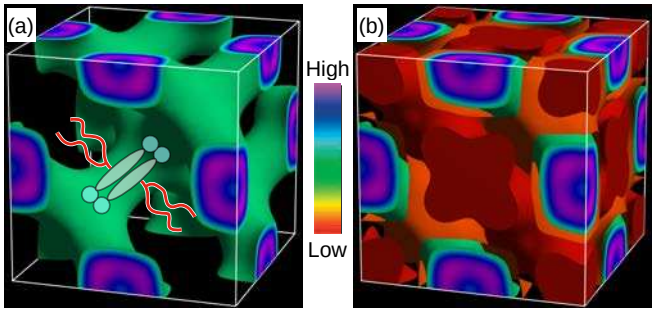

Figure 4: Reconstructed ED maps a) with the isoelectron surface enclosing (a) the high and (b) the high (green) and low (red) ED areas of the single diamond network (phase combination 0ππ000πππ0) of the *Fd*3;¯*m* phase of compound **1/18**.

In the series of compounds **1/*n***, as *n* is increased DG is replaced by SD, which is in line with the increased internetwork space made available after removing one of the networks. But why is a SD structure formed instead of the SG, or DD? To explain this we have calculated the theoretical *dV/dr* distribution curves for the DG, SG, DD, SD, DP and SP phases (Fig. 5). Here $V(r)$ is that part of the unit cell volume that is within a distance r of the closest network segment.[9,19] This dV/dr curve should match the radial distribution of side chain volume of the molecule for efficient space filling. For comparison between different phases, it is assumed that in all phases the length of the segment is the same and equal to 1. Fig. 5 shows clearly how for the double network phases DG, DD and DP, dV/dr increases with increasing r and

then decreases abruptly close to the minimum surface, where the side chains originating from the two interpenetrating networks clash. At the same time, for single network phases, while the first part is exactly the same as in the corresponding double network phases, in the second part the decrease in d*V*/d*r* happens much more gradually. For the DG structure, the *dV/dr* value drops from maximum to 0 between r = 0.6 and 0.722. This converts to 1.7 – 2.0 nm for the series of compounds discussed here, the limit that seems to be reached for side-chains in compound **1/16** whose extended length is only 2.3 nm. In contrast, the *dV/dr* curve for the SD structure is smoother and extends to larger r distances; it starts to decrease already after r = 0.4 (~1.1 nm) but drops to 0 only at r = 0.943 (~2.6 nm), allowing the accommodation of longer chains. As it happens, the extended chain length of **1/18**, the first member to adopt the SD phase, is exactly 2.6 nm. In contrast, for SG structure the *dV/dr* curve extends much further, to r_{max} = 1.299 (~3.6 nm), a distance unreachable by the side-chains of any of the compounds in the current series. Going the other way, toward shorter side-chains, by the same logic one would expect to see the DD beside DG. Indeed, a DD phase has been reported for the shortest-chain member of another series of bolaamphiphiles beside the DG phase formed by the corresponding longer homologues.[19] Overall, the d*V*/d*r* curves in Fig. 5 suggest a phase sequence DP → DD → SP → DG → SD → SG with increasing length of the side chains

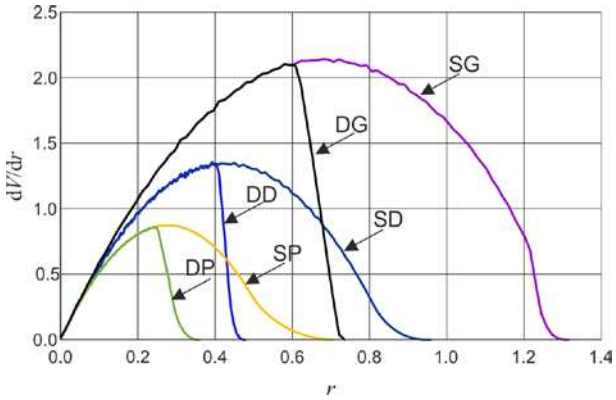

Figure 5: Radial distribution of volume functions *dV/dr* for DG, SG, DD, SD, DP and SP phases, where segment volume $V(r)$ is the volume in the unit cell that are closest to a network segment and within a distance r. The curves show the increase in occupied volume as the radius (r) of the network segments increases. For comparison between different phases the lengths of the network segments for all phases are normalized to be 1. The areas under the curves are the unit cell volumes (V_{cell}) divided by the number of network segment per unit cell (n_{cell}, see Tables S3,S4), and the molecular volume multiplied by the number of molecules per bundle. The molecular cross sectional area profile $A(r)$ should match with *dV/dr* of the considered phase for efficient space filling.

Even after adding the core radius of 0.45 nm to the 2.6 nm *all-trans* length of the **1/18**, side-chain, significant entropically unfavorable stretching is required for it to reach the distant

space around r = 2.5 nm. This manifests itself in the lowest-ED spheres (red) with reduced chain packing density in the alkyl chain continuum (Fig. 4b). The fact that the isotropization temperature T_i of the SD phase increases from 130 °C for **1/18** to 172 °C for **1/22** (Table 1) is in agreement with the stabilization of the phase in compounds with longer chains that can more easily fill the depleted distant spots in the aliphatic continuum. Noteworthy, recent coarse-grain simulations suggested a sequence SP – SD – DG upon increasing side chain volume,[26] which is different from the experimentally observed sequence in **1/*n*** and the prediction of the *dV/dr* model.

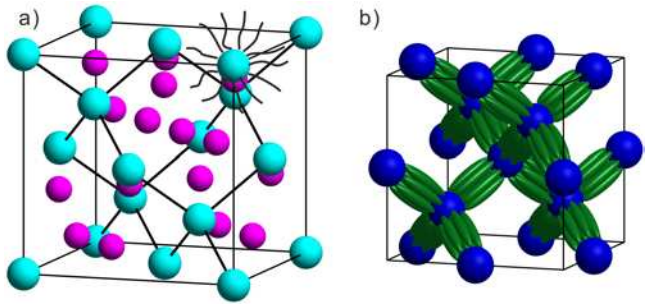

Figure 6: Models showing a) the micellar $Fd\bar{3}m$ cubic phase[27,28] and b) the new SD bicontinuous cubic phase of compounds **1/18-1/22**.

The $Fd\bar{3}m$ phase reported here (Fig. 6b) has a different structure than the previously reported $Fd\bar{3}m$ type cubic phase in lyotropic lipid systems[27] and polymers,[28] which represent the Laves C_{15} phase ($MgCu_2$-type) composed of two types of micelles (Fig. 6a). Moreover, this SD phase (Fig. 6b), as well as the DG and DD cubic rod-bundle phases (Fig. 2)[18,19] are considered to constitute a new class of cubic phases, being bicontinuous with respect to the network embedded in the continuum of lateral chains, but micellar if only the segregated polar spheres at the junctions are considered (Fig. 6b). Based on this design concept new types of single network and even more complex cubic phases can be expected in the future.[10]

Conflict of interest

There are no conflicts of interest to declare.

Acknowledgements

The work was supported by the Deutsche Forschungsgemeinschaft (392435074), EPSRC (EP-K034308, EP-P002250) and the National Natural Science Foundation of China (No. 21761132033, 21374086). We are grateful to Drs Olga Shebanova and Nick Terrill at station

I22, Diamond Light Source and Drs Jinyou Lin and Feng Tian at Beamline BL16B1 of SSRF (Shanghai Synchrotron Radiation Facility, China) for help with SAXS experiments.

References:

1 X. Cao, D. Xu, Y. Yao, L Han, O. Terasaki, S. Che, *Chem. Mater.* 2016, 28, 3691−3702; H.-Y. Hsueh, Y.-C. Ling, H.-F. Wang , L-Y. C. Chien , Y.-C. Hung , E. L. Thomas, R.-M. Ho, *Adv. Mater*. **2014**, *26*, 3225–3229; C. Y. Chu, X. Jiang, H. Jinnai, R. Y. Pei, W. F. Lin, J. C. Tsai, H. L. Chen, *Soft Matter*, **2015**, *11*, 1871–1876

2 M. Huang, C.-H. Hsu, J. Wang, S. Mei, X. Dong, Y. Li, M. Li, H. Liu, W. Zhang, T. Aida, W.-B. Zhang, K. Yue, S. Z. D. Cheng, *Science*, **2015**, *348*, 424.

3 X. Mang, X.B. Zeng, B. Tang, F. Liu, G. Ungar, R. Zhang, L. Cseh, G.H. Mehl, *J. Mater. Chem.* **2012**, *22*, 11101–11106.

4 M. Matsubara, W. Stevenson, J. Yabuki, X. Zeng, H. Dong, K. Kojima, S. F. Chichibu, K. Tamada, A. Muramatsu, G. Ungar, K. Kanie, *Chem* **2017**, *2*, 860–876.

5 W. Liu, M. Tagawa, H. L. Xin, T. Wang, H. Emamy, H. Li, K. G. Yager, F. W. Starr, A. V. Tkachenko, O. Gang, *Science* **2016**, *351*, 582-586.

6 K. Borisch, S. Diele, P. Göring, H. Kresse, C. Tschierske, *J. Mater. Chem.*, **1998**, *8*, 529–543.

7 S. Kutsumizu, *Isr. J. Chem*. **2012**, *52*, 844 – 853; C. Tschierske, *Angew. Chem. Int. Ed*. **2013**, *52*, 8828 – 8878; G. Ungar, F. Liu, X.B. Zeng, Cubic and other 3D thermotropic liquid crystal phases and quasicrystals, in *Handbook of Liquid Crystals,* 2nd Ed., Vol. 5, J.W. Goodby, P.J. Collings, T. Kato, C. Tschierske, H.F. Gleeson, and P. Raynes, eds. Wiley-VCH, Weinheim, **2014**, pp. 363–436.

8 The Scientific Graphics Project; Copyright © 1998-2004 James T. Hoffman, et. al. http://www.msri.org/publications/sgp/jim/geom/surface/global/skeletal/index.html

9 X. B. Zeng, G. Ungar, M. Imperor-Clerc, *Nat. Mater*. **2005**, *4*, 562–567.

10 M. Maldovan, A. M. Urbas, N. Yufa, W. C. Carter, E. L. Thomas, *Phys. Rev. B* **2002**, *65*, 165123.

11 M. Maldovan, E. L. Thomas, *Nat. Mater.* **2004**, *3*, 593-600.

12 V. Saranathan, C. O. Osuji, S. G. J. Mochrie, H. N. S. Narayanan, A. Sandy, E. R. Dufresne, R. O. Prum, *Proc Natl Acad. USA* **2010**, *107*, 11676–11681.

13 B. D. Wilts, K. Michielsen, H. de Raedt, D. G. Stavenga, *J. R. Soc .Interface* **2012**, *9*, 1609-1614.

14 L. Han, S. Che, *Adv. Mater*. **2018**, *30*, 1705708.

15 S. J. Richardson, M. R. Burton, P. A. Staniec, I. S. Nandhakumar, N. J. Terrill, J. M. Elliott and A. M. Squires, *Nanoscale*, **2016**, *8*, 2850–2856; M. R. Burton, C. Lei, P.A-. Staniec, N. J. Terrill, A. M. Squires, N. M. White, I. S. Nandhakumar, *Sci. Rep*. **2017**, *7*, 6405

16 S. Akbar, J. M. Elliott, M. Rittman, A. M. Squires, *Adv. Mater*. **2013**, 25, 1160–1164.

17 A. J. Meuler, M. A. Hillmyer, F. S. Bates, *Macromolecules* **2009**, *42*, 7221–7250.

18 F. Liu, M. Prehm, X. Zeng, C. Tschierske, G. Ungar, *J. Am. Soc. Chem.* **2014**, *136*, 6846–6849.

19 X. Zeng, M. Prehm, G. Ungar, C. Tschierske, F. Liu, *Angew. Chem. Int. Ed*. **2016**, 55, 8324–8327.

20 S. Poppe, C. Chen, F. Liu, C. Tschierske, *Chem Commun*. **2018**, 54, 11196-11199

21 M. Prehm, F. Liu, X. Zeng, G. Ungar, C. Tschierske, *J. Am. Chem. Soc*. **2011**, *133*, 4906–4916.

22 S. Poppe, A. Lehmann, A. Scholte, M. Prehm, X. Zeng, G. Ungar, C. Tschierske, *Nat. Commun*. **2015**, *6*, 8637.

23 M. Prehm, C. Enders, X. Mang, X. Zeng, F. Liu, G. Ungar, U. Baumeister, C. Tschierske, *Chem. Eur. J*. **2018**, *24*, 16072-16084.

24 D. R. Dukeson, G. Ungar, V. S. K. Balagurusamy, V. Percec, G. Johansson, M. Glodde, *J. Am. Chem. Soc.* **2003**, *125*, 15974-15980.

25 P. M. Duesing, R. H. Templer, J. M. Seddon, *Langmuir*, **1997**, *13*, 351-359.

26 Y. Sun, P. Padmanabhan, M. Misra, F. A. Escobedo, *Soft Matter,* **2017**, *13*, 8542—8555; A. J. Mukhtyar, F. A. Escobedo, *Macromolecules* **2018**, *51*, 9781−9788.

27 V. Luzzati, R. Vargas, A. Gulik, P. Mariani, J. M. Seddon, E. Rivas, *Biochemistry* **1992**, *31*, 279-285.

28 K.-T. Kim, M. W. Schulze, A. Arora, R. M. Lewis III, M. A. Hillmyer, K. D. Dorfman, F. S. Bates, *Science* **2017**, *356*, 520.